Clim Dyn
DOI 10.1007/s00382-013-1808-7

Climate feedback efficiency and synergy

Thorsten Mauritsen · Rune G. Graversen · Daniel Klocke · Peter L. Langen · Bjorn Stevens · Lorenzo Tomassini

Received: 21 July 2012 / Accepted: 14 May 2013

Abstract Earth's climate sensitivity to radiative forcing induced by a doubling of the atmospheric CO_2 is determined by feedback mechanisms, including changes in atmospheric water vapor, clouds and surface albedo, that act to either amplify or dampen the response. The climate system is frequently interpreted in terms of a simple energy balance model, in which it is assumed that individual feedback mechanisms are additive and act independently. Here we test these assumptions by systematically controlling, or locking, the radiative feedbacks in a state-of-the-art climate model. The method is shown to yield a near-perfect decomposition of change into partial temperature contributions pertaining to forcing and each of the feedbacks. In the studied model water vapor feedback stands for about half the temperature change, CO_2-forcing about one third, while cloud and surface albedo feedback contributions are relatively small. We find a close correspondence between forcing, feedback and partial surface temperature response for the water vapor and surface albedo feedbacks, while the cloud feedback is inefficient in inducing surface temperature change. Analysis suggests that cloud-induced warming in the upper tropical troposphere, consistent with rising convective cloud anvils in a warming climate enhances the negative lapse-rate feedback, thereby offsetting some of the warming that would otherwise be attributable to this positive cloud feedback. By subsequently combining feedback mechanisms we find a positive synergy acting between the water vapor feedback and the cloud feedback; that is, the combined cloud and water vapor feedback is greater than the sum of its parts. Negative synergies surround the surface albedo feedback, as associated cloud and water vapor changes dampen the anticipated climate change induced by retreating snow and ice. Our results highlight the importance of treating the coupling between clouds, water vapor and temperature in a deepening troposphere.

Keywords Climate sensitivity · Climate feedback mechanisms · Synergy

1 Introduction

The Earth's climate system tends towards a state of balance between the absorbed fraction of the incoming solar radiation and the emitted terrestrial radiation. This system changes its climate in response to, e.g., altered atmospheric composition or shifts in the solar input, which offset the energy balance. An increase in the atmospheric carbon dioxide (CO_2), a greenhouse gas, reduces the emitted infrared radiation, yielding a positive energy imbalance at the top of the atmosphere (TOA), i.e. the radiated energy is no longer sufficient to offset the energy absorbed. The resulting accumulation of heat in the Earth system will eventually increase the temperature, thereby increasing the emitted infrared radiation such that a new balance is

T. Mauritsen (✉)
Max Planck Institute for Meteorology, Bundesstrasse 53, 20146 Hamburg, Germany
e-mail: thorsten.mauritsen@zmaw.de

R. G. Graversen
Department of Meteorology, Stockholm University, Stockholm, Sweden

D. Klocke
European Centre for Medium Range Weather Forecasts, Reading, UK

P. L. Langen · B. Stevens · L. Tomassini
Danish Meteorological Institute (DMI), Copenhagen, Denmark

Published online: 29 May 2013

approached. The amount by which the Earth system must change its temperature in order to obtain energy balance is known as the climate sensitivity with respect to a certain forcing.

Climate sensitivity is an uncertain quantity, and in summarizing what we know from observations and climate models, the IPCC Fourth Assessment Report states a likely range of 2 to 4.5 K with respect to a doubling of atmospheric CO_2 from pre-industrial concentrations (Solomon et al. 2007). The sources of this uncertainty is of general interest, and a number of approaches to the problem have been developed in the past. Central to the current conceptual understanding of climate sensitivity is a box-model of the Earth's energy balance, in which radiative forcing and a set of feedback mechanisms together determine climate sensitivity. This conceptual framework has stood the test of time, and is widely used in the climate research community (e.g. Arrhenius 1896; Manabe and Wetherald 1967; Solomon et al. 2007), although recently alternatives have been proposed (Lu and Cai 2009; Held and Shell 2012; Ingram 2013). The purpose of this study is to explore two of the assumptions inherent to this framework, namely that the feedback mechanisms can be added and that they act independently. Possible non-linearities due to state-dependencies of the feedback mechanisms, which become relevant typically when models are forced harder with e.g. quadrupled CO_2 (Jonko et al. 2012; Block and Mauritsen 2013) are beyond our scope.

The feedback mechanisms couple the radiation balance to the surface temperature change, most notably the temperature feedback is negative as warmer temperatures lead to increasing infrared emission to space. The strength of the temperature feedback depends on the vertical structure of the warming: If the upper troposphere warms faster than the surface, then the resulting surface temperature change is smaller for a given forcing, because the Earth thereby radiates more efficiently to space. It is therefore customary to divide the temperature feedback into the Planck feedback, which is the radiation response to a vertically uniform change in tropospheric temperature equalling the surface temperature change, and the lapse-rate feedback which is the deviation from vertically uniform warming. If no other feedbacks than the temperature feedback existed, the climate sensitivity would be about 1 K with respect to a doubling of CO_2. However, in a warmer climate the atmosphere may also contain more water vapor, and because water vapor is itself a greenhouse gas, this yields the positive water vapor feedback, which is thought to roughly double the climate sensitivity (Manabe and Wetherald 1967; Schneider et al. 1999; Held and Soden 2000; Held and Shell 2012). Clouds may respond to climate change through a series of cloud feedbacks, the strength and sign of which is not well known. Further, snow- and sea ice covers retreat in a warming climate increasing the absorption of sunlight leading to further warming thereby constituting the positive surface albedo feedback, typically estimated to be an order of magnitude smaller than the water vapor feedback (e.g. Colman 2003). On longer timescales glaciers and ice sheets may form or collapse in response to climate change, augmenting the faster surface albedo feedbacks, and the ocean circulation and biogeochemical processes play a role.

Numerous diagnostic methods have been applied to determine the strength of the individual climate change feedback mechanisms in climate models. Frequently, an unperturbed model state is compared to a state obtained after the model has equilibrated with an applied forcing. Off-line radiation calculations can then be used to estimate feedbacks by systematically replacing state variables from the two equilibrium climate states (partial radiation perturbation method, PRP, Wetherald and Manabe 1988; partial radiation perturbation method, PRP, Colman and McAvaney 1997), or one can apply a more computationally efficient technique whereby mean changes in the state variables are multiplied by radiative kernels, which linearize the radiative fluxes about the basic state (Soden et al. 2008). Instead of comparing before and after states, Gregory et al. (2004) studied how a climate model approaches equilibrium after a forcing has been instantaneously applied. By regressing radiative fluxes on the changing surface temperature, and assuming that processes that operate independently of global mean surface temperature also act much more rapidly, it is possible to separate temperature-dependent effects (feedbacks) from fast adjustments, e.g., stratospheric adjustment and fast cloud response to CO_2 (Gregory and Webb 2008; Colman and McAvaney 2011; Block and Mauritsen 2013). An advantage of diagnostic methods is that they can be applied across models after they have been run according to a specified protocol facilitated by large model intercomparison projects. Frequently, such intercomparison studies find that the major contributor to uncertainty in climate sensitivity is cloud feedbacks (Cess et al. 1990; Colman 2003; Soden and Held 2006; Dufresne and Bony 2008; Soden et al. 2008; Vial et al. 2013; Webb et al. 2013), while some studies find less pronounced cross-model variability in the cloud feedback (Gregory and Webb 2008; Crook et al. 2011).

Underlying these diagnostic methods are the assumptions of additivity and independence of the feedback mechanisms; that each feedback is assumed to be equally effective in contributing to climate change and depend only on the global mean surface temperature change. The validity of these assumptions can be tested in climate models by performing experiments with one or more of the radiative feedbacks disabled, locked or imposed, thereby

allowing an attribution of the change in the radiative fluxes to the change in state.

Feedbacks can be locked by prescribing for instance surface albedo, clouds or water vapor in the model radiation calculations to a climatology or states stored from another run. For example, Cess et al. (1991) compared snow feedbacks in an ensemble of atmosphere-only models with prescribed SST and sea ice, finding a vast range of responses ranging from even slightly negative to strongly positive. The cause of the large inter-model spread was not so much due to variation in the snow albedo feedback itself, but rather due to the interactions with clouds, water vapor and temperature feedbacks (Randall et al. 1994). Apart from this early model intercomparison study, most other studies that we are aware of are limited to single models: Wetherald and Manabe (1988) find that cloud feedbacks increase the climate sensitivity from 3.2 to 4.0 K in their model, mainly due to Tropical cirrus clouds rising with the tropopause in a warming climate, thereby reducing the terrestrial radiation to space. This was in qualitative agreement with a radiative-convective equilibrium model study by Augustsson and Ramanathan (1977) finding a sensitivity of 1.98 K when clouds are kept at constant height, and 3.2 K when held at constant temperature. The resulting cloud feedback mechanism was later to become rationalized as the fixed anvil temperature (FAT) hypothesis (Hartmann and Larson 2002), and it has come to be one of the more robust cloud responses across models (Zelinka and Hartmann 2010). Hall and Manabe (1999) locked the water vapor in a climate model finding that the feedback more than tripled global mean climate sensitivity. In contrast, Schneider et al. (1999) suppressed both cloud- and surface albedo feedbacks in a model, and found that water vapor feedback merely doubles climate sensitivity when acting in isolation. Hall (2004) compared a climate model with free and locked surface albedo and found that the surface albedo feedback increases climate sensitivity pertaining to a CO_2-doubling by about 1 K and, somewhat surprisingly, with a 20 percent increased warming in the tropics. Graversen and Wang (2009), on the other hand, found an increase in global climate sensitivity of only 0.26 K and practically no impact on the tropics originating from the surface albedo feedback.

In the present study we shall test the assumptions of additivity and independence of climate change feedback mechanisms. We do so by systematically controlling the surface albedo, cloud and water vapor feedbacks in a state-of-the-art climate model. Thereby, we obtain effective feedback estimates based on the temperature response associated with each feedback mechanism. In addition, we diagnose the feedback factors offline using the accurate, but computationally expensive partial radiation perturbation method (PRP). The extent to which these various estimates of effective and diagnosed feedbacks agree, or disagree, determines the validity of the assumptions.

2 Feedback analysis

Climate feedback factors can be linked to partial temperature contributions following Dufresne and Bony (2008). Consider a climate system which is in a radiative balance between the absorbed solar radiation and terrestrial radiation emitted to space. The system is then perturbed by an external forcing, F, that initially will offset the radiation balance at the top of the atmosphere by an equal amount, ΔR. The system will then warm and eventually restore the radiation balance after changing its global mean surface temperature by an amount ΔT. We can linearize the problem to:

$$\Delta R = F + \lambda \Delta T \tag{1}$$

and if we assume that the system consists of a finite set of additive and mutually independent feedback mechanisms we can for instance decompose the feedback factor (λ):

$$\lambda = \lambda_T + \lambda_W + \lambda_C + \lambda_A$$

into the sum of the temperature (λ_T), water vapor (λ_W), cloud (λ_C) and surface albedo (λ_A) feedback factors. The conceptual framework described by Eq. 1) is illustrated in Fig. 1a). The total feedback factor, λ, must be negative to yield a stable climate system, and can be estimated from the equilibrium response and the strength of the forcing:

$$\lambda = -\frac{F}{\Delta T}. \tag{2}$$

The temperature feedback is considered here to play a special role in the climate system because it is the main restoring mechanism of the radiation balance. While the other feedbacks are positive in the cases of the water vapor feedback and the surface albedo feedback, and either positive or negative in the case of the cloud feedback, the temperature feedback is strongly negative because blackbody radiation is proportional to the temperature raised to the fourth power. If one were to, somehow, disable the temperature feedback then the resulting climate system would be unstable because the total feedback factor would be rendered positive.

In a case where the water vapor, cloud and surface albedo feedbacks are not active, we obtain $\lambda = \lambda_T$ (Fig. 1b). If we then assume that the forcing is the same as before, we can estimate λ_T given the forcing and the partial temperature response to forcing in the absence of feedbacks (ΔT_F):

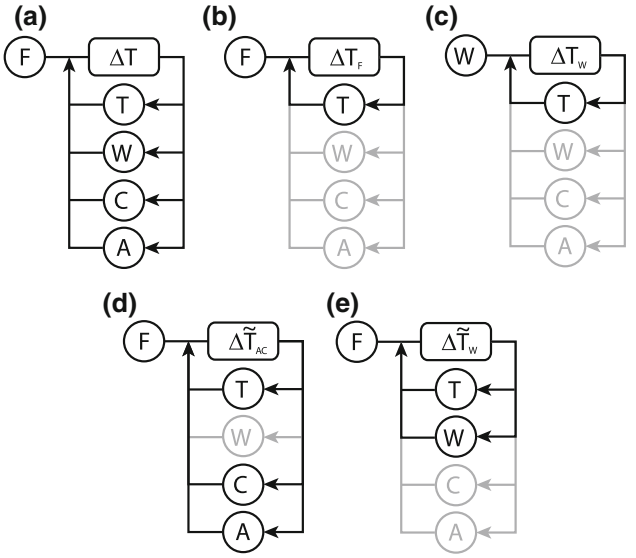

Fig. 1 Illustration of a conceptual climate system with **a** feedbacks due to changes in temperature (T), water vapor (W), clouds (C) and surface albedo (A). The system responds to external forcing (F) by changing its temperature (ΔT). System **b** has the water vapor, cloud and surface albedo feedbacks disabled, while system **c** imposes the water vapor feedback from the fully equilibrated system in a) as if it was a forcing. System **d** allows both the cloud and surface albedo feedbacks to act in response to the temperature change, whilst keeping the atmospheric water vapor fixed. System **e** has the water vapor feedback enabled, while clouds and surface albedo are prescribed

$$\lambda_T = -\frac{F}{\Delta T_F}. \tag{3}$$

Figure 2 displays the relation between the feedback factors and climate sensitivity for the full system with positive feedbacks and with only temperature feedback. Although the conceptual framework we adopt is assumed to be additive and independent in the feedback factors, climate sensitivity (ΔT) is inversely proportional to the total feedback factor (λ), which is crucial to appreciating the behavior of models with locked feedbacks. In the following we shall first connect the feedback factors pertaining to each mechanism to the partial temperature contributions of the full response of the system, second derive expressions to connect the response for combinations of feedback mechanisms to their feedback factors.

2.1 Imposed feedbacks and partial temperature contributions

Consider now a system where we impose a feedback, for example the water vapor feedback (Fig. 1c). We can do so by prescribing the water vapor fields obtained from the full climate system to radiation in the feedback-free system (Fig. 1a). Strictly speaking, the imposed water vapor

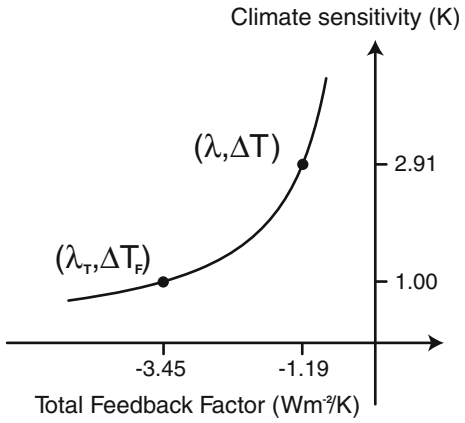

Fig. 2 The relation between total feedback factor and equilibrium climate sensitivity for a doubling of CO_2 following Eqs. (2) and (3). The *two dots* correspond to a system with only temperature feedback $(\lambda_T, \Delta T_F)$ and a full system $(\lambda, \Delta T)$ with additional positive feedbacks. The *numbers* are derived for the ECHAM6 climate model, the subject of this study (Sect. 4)

feedback is then no longer a true feedback in the sense that it does not depend on the actual climate system state. Instead, the imposed water vapor perturbation can be considered a kind of forcing that acts on the climate system by initially offsetting the radiation balance by an amount $\Delta R_W = \lambda_W \cdot \Delta T$, while the climate system responds by changing its temperature by an amount ΔT_W to satisfy:

$$\lambda_W \cdot \Delta T = -\lambda_T \cdot \Delta T_W,$$

from which we isolate the effective water vapor feedback factor:

$$\lambda_W = -\lambda_T \frac{\Delta T_W}{\Delta T}. \tag{4}$$

Analogous expressions for the cloud and surface albedo feedback factors can be readily obtained. By inserting Eqs. (3) and (4) into Eq. (2) it can further be shown that the sum of the imposed feedback responses is to yield the full response to the forcing:

$$\Delta T = \Delta T_F + \Delta T_W + \Delta T_C + \Delta T_A, \tag{5}$$

that is, the method of imposing feedbacks must yield a meaningful linear separation of the partial temperature contributions to climate change from each feedback mechanism. Note that ΔT_F is the temperature response to the forcing in the absence of the water vapor, cloud and surface albedo feedbacks.

2.2 Feedback locking and interacting feedback combinations

Now, consider climate systems where we enable one feedback at a time. Figure 1e illustrates a system with the water vapor feedback enabled. Hence the water vapor

feedback is free to act, while the cloud and surface albedo feedbacks are locked to the CTRL-state. Let $\Delta\widetilde{T}_W$ be the equilibrium temperature response to the forcing F of this particular climate system, then we obtain an estimate of the water vapor feedback factor:

$$\lambda_W = -\left(\lambda_T + \frac{F}{\Delta\widetilde{T}_W}\right). \quad (6)$$

Further, using the climate system with the surface albedo and the cloud feedback mechanisms enabled, and water vapor locked (Fig. 1d), we can obtain an estimate of their combined feedback factor (λ_{AC}):

$$\lambda_{AC} = -\left(\lambda_T + \frac{F}{\Delta\widetilde{T}_{AC}}\right). \quad (7)$$

This particular system was compared to the full system by Hall and Manabe (1999) to study the role of the water vapor feedback.

Note that it is not to be expected that the difference between the original climate system and the system with e.g. the water vapor feedback disabled ($\Delta T - \Delta\widetilde{T}_{AC}$) equals the water vapor partial temperature response (ΔT_W), because the surface albedo and cloud feedbacks can act to strengthen or weaken the response in the former case, even in the simple conceptual framework (Fig. 2). However, if the feedbacks are additive and independent in the sense that they only depend on the global mean surface temperature change, then we expect the estimated feedback factors to be independent of how they were estimated (Eqs. 4, 6 or 7). This will be explored in Sect. 4.

3 Model, experiments and methods

We use a modified version of the Max Planck Institute (MPI) for Meteorology atmospheric model ECHAM6 version 6.0 at T63 horizontal resolution with 47 vertical levels (Stevens et al. 2013). ECHAM6 at this resolution comprises the atmosphere and land components of the MPI Earth System Model at Low Resolution (MPI-ESM-LR, Giorgetta et al. 2013) used in the fifth phase of the Coupled Model Intercomparison Project (CMIP5, Taylor 2012). In the present study ECHAM6 is coupled to a 50 m deep mixed-layer ocean, instead of the full three-dimensional ocean component used in MPI-ESM-LR. Ocean heat transport is inferred from the monthly mean surface fluxes in a 30-year simulation with prescribed observed sea surface temperatures and sea ice concentrations following the Atmospheric Model Intercomparison Project (AMIP) protocol. The ocean heat transport does not change from year to year, nor between simulations. The mixed-layer ocean model component forms sea ice, though it is not being advected and does not deform.

3.1 Locking feedbacks in ECHAM6

The ECHAM6 model is modified such that the radiative water vapor, cloud and surface albedo feedbacks can be locked or imposed. This is done by first writing out all relevant instantaneous fields at every 2-hourly radiation call during entire simulations where the model is run in the standard configuration wherein all the feedbacks are fully interactive, or free. These runs are carried out with CO_2 at pre-industrial levels (284.7 ppm) and doubled concentration (569.4 ppm). Subsequently, simulations are performed where select fields from these free runs are read into the models radiation calculations at every radiation call at the same time of day and year, in the same way as it was also done by Langen et al. (2012) in another model. The approach allows us to sample the full inter-annual variability of the model, and at the same time to compensate for space-time correlation effects when multiple fields are read from the same run by reading each field from different years. Other studies have used fields from single years repeatedly (Schneider et al. 1999), an annual cycle averaged from multiple years (Hall and Manabe 1999; Hall 2004; Graversen and Wang 2009), or a small set of cloud scenes (Wetherald and Manabe 1988).

The same basic methodology is used for all three feedbacks, although the surface albedo scheme of ECHAM6 required special considerations as described below. The water vapor feedback is disabled by simply replacing the model's actual three-dimensional specific humidity field in the call to radiation. The cloud feedback is likewise controlled by replacing the cloud fraction, cloud liquid, cloud ice and cloud droplet number concentration in the call to radiation. It is important to note that we do not replace the model's prognostic water vapor and cloud fields, hence the modified model has internally consistent energy and hydrological cycles.

The surface albedo in ECHAM6 is calculated from the land, ocean and sea ice albedo, and is further treated separately for visible and near-infrared, and for direct and diffuse light. The surface albedo fields are updated at each time step and aggregated to a grid-cell mean albedo. The open ocean albedo depends on the solar zenith angle and the fraction of diffuse- to direct sunlight. The latter is controlled mainly by clouds, and hence changes in ocean albedo may either be considered a pure surface albedo feedback, or as part of the cloud feedback. We chose to let the model calculate an ocean albedo that is consistent with the prescribed cloud fields. As we shall see later this leads to a slightly enhanced global mean surface albedo feedback. Further complication arises because the actual fraction of sea ice is not necessarily the same as in the saved fields from the free runs at any given instance. Therefore, in order to have the sea ice influence the grid-cell

Table 1 Overview of simulations. For the surface albedo, cloud and water vapor radiative feedbacks, the relevant fields are read '1' either from CTRL (284.7 ppm) or '2' from 2xCO_2 (569.4 ppm)

Simulation name	CO_2	Surface Albedo	Cloud	Water vapor	# Years
CTRL	1				50
2xCO_2	2				50
1xCO_2-A1C1W1	1	1	1	1	25
1xCO_2-A2C1W1	1	2	1	1	25
1xCO_2-A1C2W1	1	1	2	1	25
1xCO_2-A1C1W2	1	1	1	2	25
1xCO_2-A2C2W1	1	2	2	1	25
1xCO_2-A1C2W2	1	1	2	2	25
1xCO_2-A2C1W2	1	2	1	2	25
1xCO_2-A2C2W2	1	2	2	2	25
2xCO_2-A1C1W1	2	1	1	1	25
2xCO_2-A2C1W1	2	2	1	1	25
2xCO_2-A1C2W1	2	1	2	1	25
2xCO_2-A1C1W2	2	1	1	2	25
2xCO_2-A2C2W1	2	2	2	1	25
2xCO_2-A1C2W2	2	1	2	2	25
2xCO_2-A2C1W2	2	2	1	2	25
2xCO_2-A2C2W2	2	2	2	2	25
1xCO_2-A1	1	1			45
2xCO_2-A1	2	1			45
1xCO_2-C1	1		1		45
2xCO_2-C1	2		1		45
1xCO_2-W1	1			1	45
2xCO_2-W1	2			1	45
1xCO_2-A1C1	1	1	1		45
2xCO_2-A1C1	2	1	1		45
1xCO_2-A1W1	1	1		1	45
2xCO_2-A1W1	2	1		1	45
1xCO_2-C1W1	1		1	1	45
2xCO_2-C1W1	2		1	1	45
1xCO_2-SST	1				20
2xCO_2-SST	2				20
1xCO_2-A1C1W1-SST	1	1	1	1	20
2xCO_2-A1C1W1-SST	2	1	1	1	20
1xCO_2-A1C1-SST	1	1	1		20
2xCO_2-A1C1-SST	2	1	1		20
1xCO_2-A1W1-SST	1	1		1	20
2xCO_2-A1W1-SST	2	1		1	20
1xCO_2-C1W1-SST	1		1	1	20
2xCO_2-C1W1-SST	2		1	1	20

No value means the feedback is free. Runs with 'SST' at the end of their name have sea surface temperatures and sea ice concentration read from CTRL. The first large set of simulations have feedback systematically imposed, the second group has either one or two feedback locked, while the third group is used to estimate adjusted CO_2 forcing

aggregated albedo in the same way as in the free runs, it was chosen to modify the albedo of the open ocean and sea ice: If for instance a grid cell was fully covered by sea ice, but the saved fields indicated that no sea ice was present in the free run, then the albedo of the sea ice was set to that of the open ocean. Vice-versa, if more ice was present in the saved fields than in the actual model state, the ocean albedo was increased in such a way as to yield the area averaged surface albedo as if more ice had been present. Again, it is important to note that the model has its own sea-ice and snow covers, which can freeze and melt and thereby influence the temperature by releasing latent heat of fusion; it is only the influence of snow and ice on the surface albedo that is being imposed.

3.2 Overview of simulations

To systematically sample the different ways feedbacks can be imposed or locked requires a large number of simulations. An overview of the simulations prepared for this study is provided in Table 1 and the temperature evolution of a subset of simulations is shown in Fig. 3.

ECHAM6 was first spun up with pre-industrial CO_2 for 50 years to reach stationarity, then two simulations named CTRL and 2xCO_2 were performed starting from this state. These were each 50 years long, and all relevant data for locking feedbacks were saved. Subsequently, a simulation named 'spinup' with pre-industrial CO_2 and feedbacks locked to CTRL was performed for 15 years. It is seen that locking feedbacks results in a slight warming of about 0.2 K. The model state at the end of this spin-up run served as the starting point for the subsequent set of 16 runs with imposed feedbacks and CO_2 in different configurations. For these runs the nomenclature is such that the name of each run first indicates the CO_2 concentration, then letters and numbers follow indicating whether the surface albedo (A), cloud (C) and water vapor (W) were read from either CTRL (1), or imposed from the 2xCO_2 run (2). For example, the simulation 2xCO_2-A2C1W1 is a simulation with doubled CO_2 in which the surface albedo fields are imposed from the 2xCO_2 simulation and the clouds and water vapor are imposed from the CTRL simulation. This group of 16 simulations are relevant for deriving partial temperature contributions associated with each feedback and for investigating feedback efficiency (Sects. 2.1 and 4.2). The following group of 12 simulations in Table 1 had either one or two feedbacks locked to the CTRL simulation, as indicated by their names. These simulations are relevant for estimating feedback synergies (Sects. 2.2 and 4.3).

The remaining ten simulations ending with 'SST' have prescribed monthly mean sea ice and sea surface temperatures obtained from the CTRL run. These simulations are

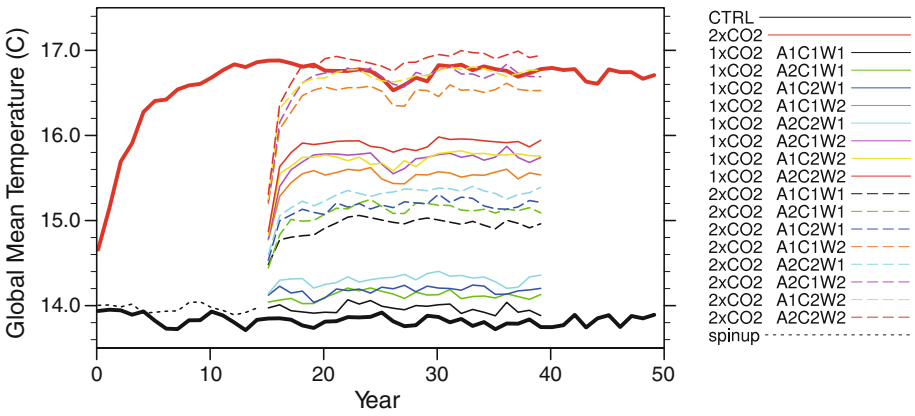

Fig. 3 Global mean surface air temperature evolution for free- and imposed feedback experiments. The experiment labels are explained in the text

used to estimate adjusted CO_2-forcing, F_s (Hansen et al. 2005):

$$F_s = \Delta R_o - \lambda \cdot \delta T_o \tag{8}$$

where ΔR_o is the change in TOA radiation balance, for instance between 2xCO_2-SST and 1xCO_2-SST, and δT_o is the small change in surface air temperature that occurs because the land temperatures are not held fixed. Unlike Hansen et al. (2005) who used a prescribed value for λ, we determine the feedback factor from the slope between adjusted state $(\delta T_o, \Delta R_o)$ and the near-equilibrium state $(\Delta T, \delta R)$, where δR is the small remaining TOA radiation imbalance. This choice introduces uncertainty in the forcing estimate, as it is not obvious that the feedback factor is the same for the land-only and global warmings.

3.3 Methodological concerns

The changes made to the climate model in this and in previous studies dealing with imposing or locking feedbacks are intrusive to the model as it will be run in unphysical states, and one might rightfully be concerned how to interpret the results physically. For example, the model might simulate a storm while the radiation code sees only clear skies, or there may be open ocean where the radiation sees sea ice.

There exist natural spatial correlations between clouds and water vapor, so if the model is first run with correlated fields in one configuration (e.g. A1C1W1) and then with de-correlated fields in another configuration (e.g. A1C1W2), a spurious radiative forcing may occur that adds artificially to the response. Therefore we de-correlate the water vapor, cloud and surface albedo fields by reading them from different years of CTRL and 2xCO_2. Thereby we avoid spurious de-correlation effects, as discussed extensively by Schneider et al. (1999) and Langen et al. (2012). The need to account for spatial correlation-effects is also relevant to widely accepted diagnostic methods (Colman and McAvaney 1997).

Another concern is if the method leads to a significantly different control climate. Schneider et al. (1999) studied this problem in detail, finding for instance that the base climate warms by 0.5 K, if one only locks the water vapor feedback. We can confirm their result, as our model warms by 0.8 K in this particular configuration (1xCO_2-W1 minus CTRL). Yet, this base-state temperature change is small relative to the total change from doubling CO_2, around 3 K, and further, when doubling CO_2 without water vapor feedback the absolute global mean temperature is still less than that in the 2xCO_2 run; base state warming of 0.8 K plus 1.21 K of climate change as to be shown later in Fig. 5. When instead imposing all feedbacks the control climate shift is limited to 0.2 K (Fig. 3, 1xCO2-A1C1W1 minus CTRL), and as we shall see in Sect. 4 estimates of partial temperature contributions in this setup are practically independent of background state.

Although care must be taken when interpreting results obtained by the online feedback method, the method's perhaps greatest asset in the context used here is that the simulations with imposed feedbacks fulfill Eq. (5), showing that a meaningful decomposition of the total temperature change into partial temperature contributions from the individual feedback mechanisms has been achieved. Both regionally and in the zonal averaged vertical structure the difference is usually less than 0.2 K (Fig. 4), and similar properties are found for variables such as sea-level pressure, precipitation and energy transport (not shown). Interestingly, this may imply that the gross features of the modeled circulation change are determined almost entirely by the structure of the radiative perturbations from CO_2, water vapor, clouds and surface albedo, and hence, that space and time correlations associated with synoptic variability are not important for aspects relevant to the present study.

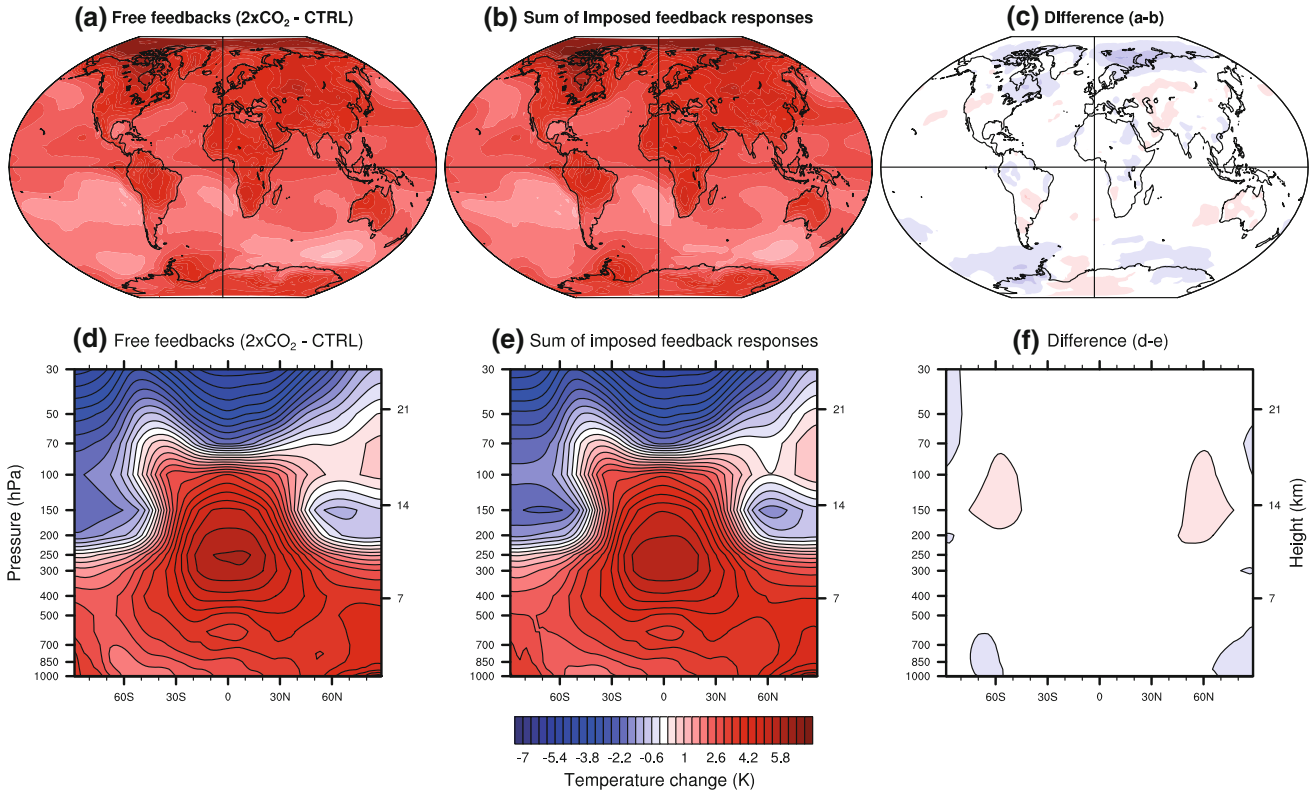

Fig. 4 Structure of surface air temperature and the vertical structure of temperature change from standard simulations, the sum of the feedback contributions (Eq. 5), and the difference. The minimum contour level is at ±0.2 K and the contour spacing is 0.4 K

3.4 Diagnostic feedback estimates

The partial radiation perturbation (PRP) diagnostic method makes use of a radiative transfer code to estimate the strength of the feedbacks after a model has been run by systematically replacing the relevant fields between CTRL and $2xCO_2$ (Wetherald and Manabe 1988; Colman and McAvaney 1997). Details of the method used here is given in Klocke et al. (2013). Here we apply the radiation code that is also used in ECHAM6 itself. The evaluation of the feedbacks are done over the last twelve years (38-49), of the simulations on the basis of the model's 6-hourly output, to average out interannual variability which is particularly important for estimating the cloud feedback (Klocke et al. 2013).

The temperature feedback is evaluated by replacing the surface and atmospheric temperatures below the tropopause. Here the tropopause is defined as the lowest level at which the lapse rate decreases to 2 K/km or less, provided the average lapse rate between this level and all higher levels within 2 km does not exceed 2 K/km (WMO 1992). First, the temperature fields in the CTRL-state are replaced by the $2xCO_2$ temperatures, and the TOA radiative fluxes compared with those obtained in the CTRL-state. Then, the flux perturbation is calculated in the $2xCO_2$-state by replacing the temperatures with those from the CTRL-state. The average of the two estimates is finally divided by the equilibrium surface temperature change to yield the diagnosed temperature feedback factor. The cloud and the water vapor feedback factors are evaluated in the same way as the temperature feedback.

In estimating the surface albedo feedback we use the effective surface albedo calculated from the downwelling and reflected shortwave surface fluxes, both of which are averaged over the 6-hour output intervals. There is a slight increase in the ocean albedo in the warm climate, because cloudiness is reduced in the tropics and sub-tropics yielding a larger fraction of direct relative to diffuse sunlight. Excluding the impact of open ocean albedo change increases the global mean estimate of the surface albedo feedback factor from 0.16 to 0.20 W m^{-2} K^{-1}.

4 Results

The results of the climate simulations are summarized in Fig. 5. The climate sensitivity of the standard ECHAM6 model is 2.91 K, with respect to a CO_2-doubling starting from pre-industrial levels, while the other bars show the model response in the various configurations sketched in

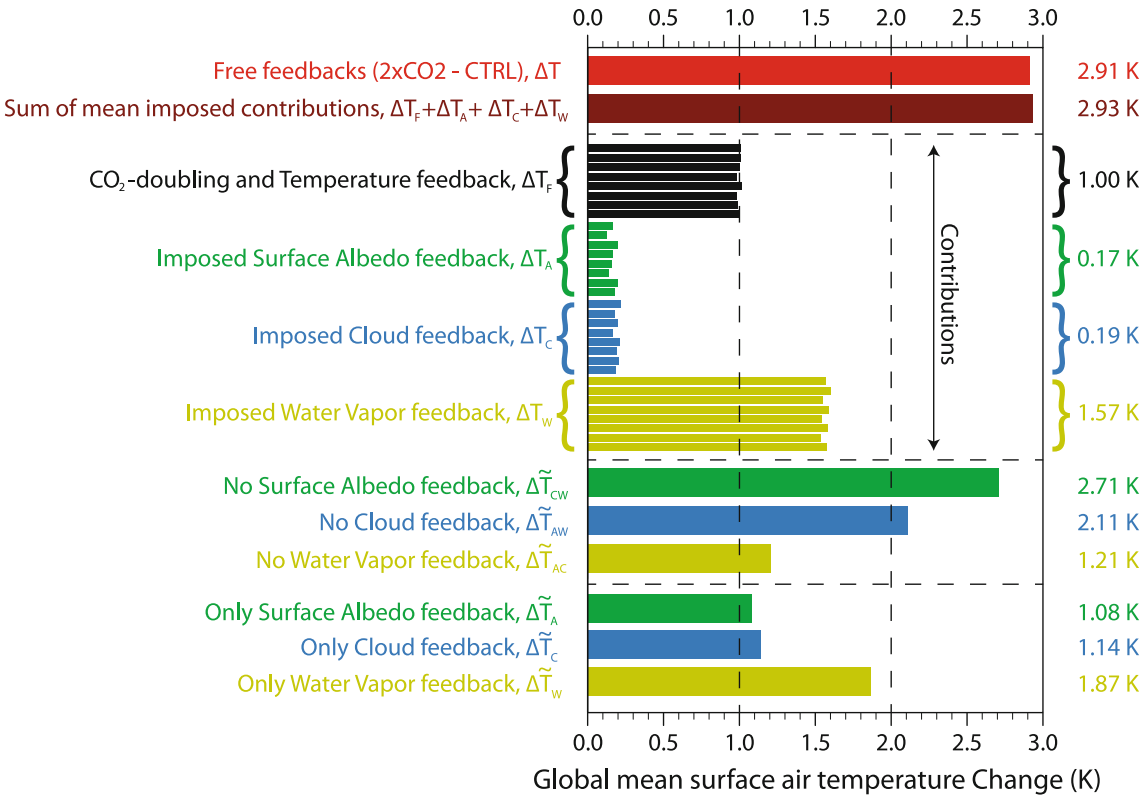

Fig. 5 *Red bar* shows the near-equilibrium climate change pertinent to a doubling of CO_2 in ECHAM6 with free feedbacks ($2xCO_2$ minus CTRL). *Brown* is the sum of the four contributions from CO_2 forcing (*black*) and the surface albedo (*green*), cloud (*blue*) and water vapor (*yellow*) feedbacks. The *lower six bars* show the temperature change to a doubling of CO_2 in climate systems with one or two feedbacks locked at a time

Fig. 1. The model setups in Fig. 1b, c allow us to break the climate response into partial temperature contributions. There are eight individual estimates obtained from pairs of simulations with only one particular imposed feedback differing. For example, $1xCO_2$-A2C1W1 minus $1xCO_2$-A1C1W1 provides one estimate of the albedo feedback response at temperatures close to the control climate, while $2xCO_2$-A2C2W2 minus $2xCO_2$-A1C2W2 provides another estimate, albeit in a warmer state. Overall, there is little variation between the eight individual estimates for each contribution, indicating that within this temperature range feedbacks are not state-dependent.

The doubling of CO_2 in the absence of feedbacks leads to a warming of 1.00 K, imposing the water vapor feedback contributes 1.57 K warming, and the surface albedo and cloud feedbacks each provide less than 0.2 K warming. Summing the four partial temperature contributions we obtain a global climate sensitivity of 2.93 K, which is very close to that of the standard ECHAM6 model, and so our model setup fulfills Eq. (5) to within 1 percent in the global mean.

Intriguingly, the simulations with only one of the feedbacks locked at a time provide a somewhat different picture concerning the relative strengths of the surface albedo and cloud feedbacks: Locking the surface albedo feedback reduces the model's climate sensitivity by 0.2 K, while it drops by 0.8 K when locking only the cloud feedback. These findings are further well in line with a global mean temperature impact of the surface albedo feedback of 0.26 K as reported by Graversen and Wang (2009), and 0.8 K for the cloud feedback as reported by Wetherald and Manabe (1988). On the contrary, Hall (2004) found a much larger impact of locking the surface albedo feedback of about 1 K globally.

Focussing on the water vapor feedback we find that when it is activated there is a factor 1.87 increase ($\Delta\widetilde{T}_W/\Delta T_F$) in climate sensitivity relative to the feedback-free CO_2-response, in good agreement with the equivalent experiment by Schneider et al. (1999). On the other hand, when the other feedbacks are free, then enabling the water vapor feedback leads to an increase in climate sensitivity by a factor 2.4 ($\Delta T/\Delta\widetilde{T}_{AC}$), which is somewhat closer to the study by Hall and Manabe (1999) finding a factor 3.2 increase using that same type of model setup. The difference in the impact of the water vapor feedback on climate sensitivity between the different setups is in qualitative

agreement with the energy balance model because climate sensitivity is inversely proportional to the total feedback factor (Fig. 2). Hence, it matters in which order feedbacks are added to the system; adding a positive feedback to a system with other feedbacks active yields a larger relative increase in climate sensitivity. These aspects will be further explored in Sect. 4.3.

4.1 Effective feedback factors

In order to convert the partial temperature contributions to effective feedback factors it is necessary to know the forcing from the CO_2-doubling. Figure 6 shows the evolution of the global mean surface air temperature and TOA imbalance as climate is equilibrating after an instantaneous CO_2-doubling. The unperturbed state is at the origin, marked 'A', and the perturbed equilibrium state as determined by the line is at 3.03 K, marked 'B'. Note that this estimate of climate sensitivity is slightly higher than the average over years 20 to 49 because it includes warming still in the pipeline corresponding to the remaining TOA radiation imbalance of 0.13 W m^{-2}, of which merely 0.03 W m^{-2} is due to a slight increase in model energy leakage, as inferred from the atmospheric energy budget. The transient towards the new equilibrium is shown as individual years, which follow closely the black line intersecting the y-axis at 'C' which is 4.35 W m^{-2}. This line is calculated using the technique for obtaining the atmospheric adjusted forcing, see Eq. (8). The difference between A and C has come to be known as the adjusted forcing, and the climate system's total feedback factor, λ, can be obtained from the slope between C and B (Gregory et al. 2004).

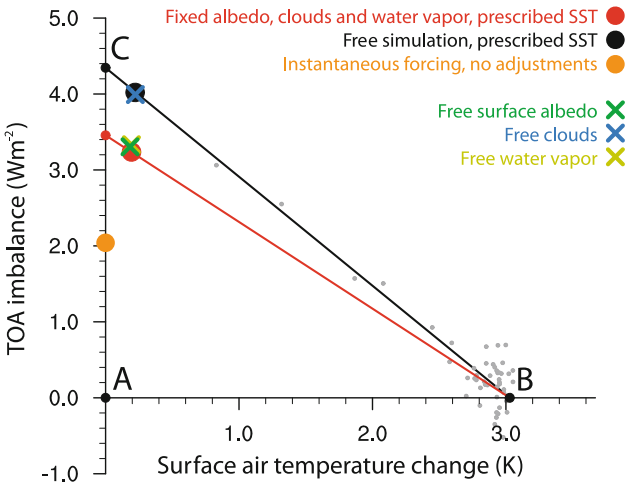

Fig. 6 Evolution of the global mean temperature and TOA radiation imbalance in ECHAM6 after an abrupt doubling of the CO_2 concentration. Small *grey dots* are individual years from the 2xCO_2 simulation. *Point A* marks the unperturbed state, while *B* is an estimated new equilibrium state and *C* is a measure of adjusted forcing. *Points B* and *C* are determined by the *black line*. *Large orange circle* is the instantaneous TOA forcing from a doubling of CO_2. *Large black dot* is the mean obtained from two runs with prescribed sea ice distribution and sea surface temperatures (2xCO_2-SST minus 1xCO_2-SST), while the *large red dot* is obtained in the same way although with clouds, surface albedo and water vapor held fixed (2xCO_2-A1C1W1-SST minus 1xCO-A1C1W1-SST). Crosses show cases were one of the surface albedo, cloud or water vapor components are allowed to respond to the change in CO_2. For example, the *blue cross* is obtained from simulations with free clouds, and prescribed water vapor, surface albedo (2xCO_2-A1W1-SST minus 2xCO_2-A1W1-SST). The *yellow cross* is behind the *green cross*

On the other hand, if one calculates the instantaneous radiative forcing from a doubling of CO_2 in ECHAM6 using the PRP method one obtains only 2.04 W m^{-2}, as marked by the orange dot. The difference between the instantaneous CO_2-forcing and the adjusted forcing at the intercept is due to relatively fast processes that occur independently of the surface temperature. It is well known that the stratosphere rapidly cools radiatively after a CO_2-doubling leading to a pronounced increase in the TOA imbalance (Hansen et al. 1997). The research community best estimate of the forcing after stratospheric adjustment is 3.7 W m^{-2} (Solomon et al. 2007). To calculate the radiative forcing in ECHAM6 we keep the surface albedo, clouds and water vapor locked to the control state and only let the atmospheric temperature change (red), yielding a y-axis intercept of 3.45 W m^{-2}. The remaining 0.9 W m^{-2} of the adjusted forcing from a doubling of CO_2 is due mainly to fast cloud adjustments that occur independently of changes in the surface temperature. We show this by systematically repeating the prescribed SST experiments while letting either surface albedo, clouds or water vapor respond (crosses). These results imply that clouds add significantly to adjusted

Table 2 Feedback factors diagnosed using various methods

Method	λ_T	λ_A	λ_C	λ_W	λ
(2xCO_2-CTRL), Eq. (2)					−1.19
PRP diagnosed feedbacks	−4.05	0.20[a]	0.63	1.98	−1.24[a]
Imposed feedback response, Eqs. (3, 4)	−3.45	0.20	0.23	1.86	
Two locked feedbacks, Eq. (6)		0.26	0.42	1.60	
		λ_{CW}	λ_{AW}	λ_{AC}	
One locked feedback, Eq. (7)		2.17	1.81	0.59	

Units are W $m^{-2}K^{-1}$. In these estimates a radiative forcing of 3.45 W m^{-2} from a doubling of CO_2 (surface albedo, clouds and water vapor held fixed), and a surface air temperature change of 2.91 K is used, which is the average of the years 20–49 of the simulations (2xCO_2 minus CTRL). [a]The surface albedo feedback estimate based on PRP is corrected for negative values over open ocean associated with cloud changes as described in Sect. 3.4. Before this correction the global mean surface albedo feedback is 0.16 W m^{-2} K^{-1}

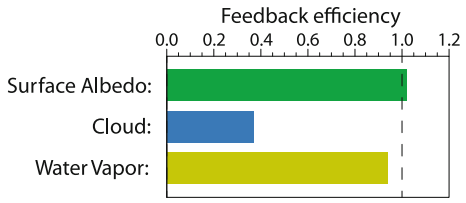

Fig. 7 Feedback efficiencies in ECHAM6 calculated as the ratio of the effective feedback factors derived from responses to imposed feedbacks to diagnosed PRP feedback factors shown in Table 2. The corrected value for the PRP surface albedo feedback is used

forcing. However, in the present study we impose or lock the clouds to either the unperturbed equilibrium state A, or the perturbed equilibrium state B. Hence, we do not distinguish between the cloud feedback and contributions from cloud adjustments to forcing, and so in the subsequent analysis we use the radiative forcing, 3.45 W m^{-2}, rather than the larger adjusted forcing. Note that the choice of λ in Eq. (8) may lead to a slight underestimation of the radiative forcing, and therefore also of the effective feedback factors (Eqs. 3, 4).

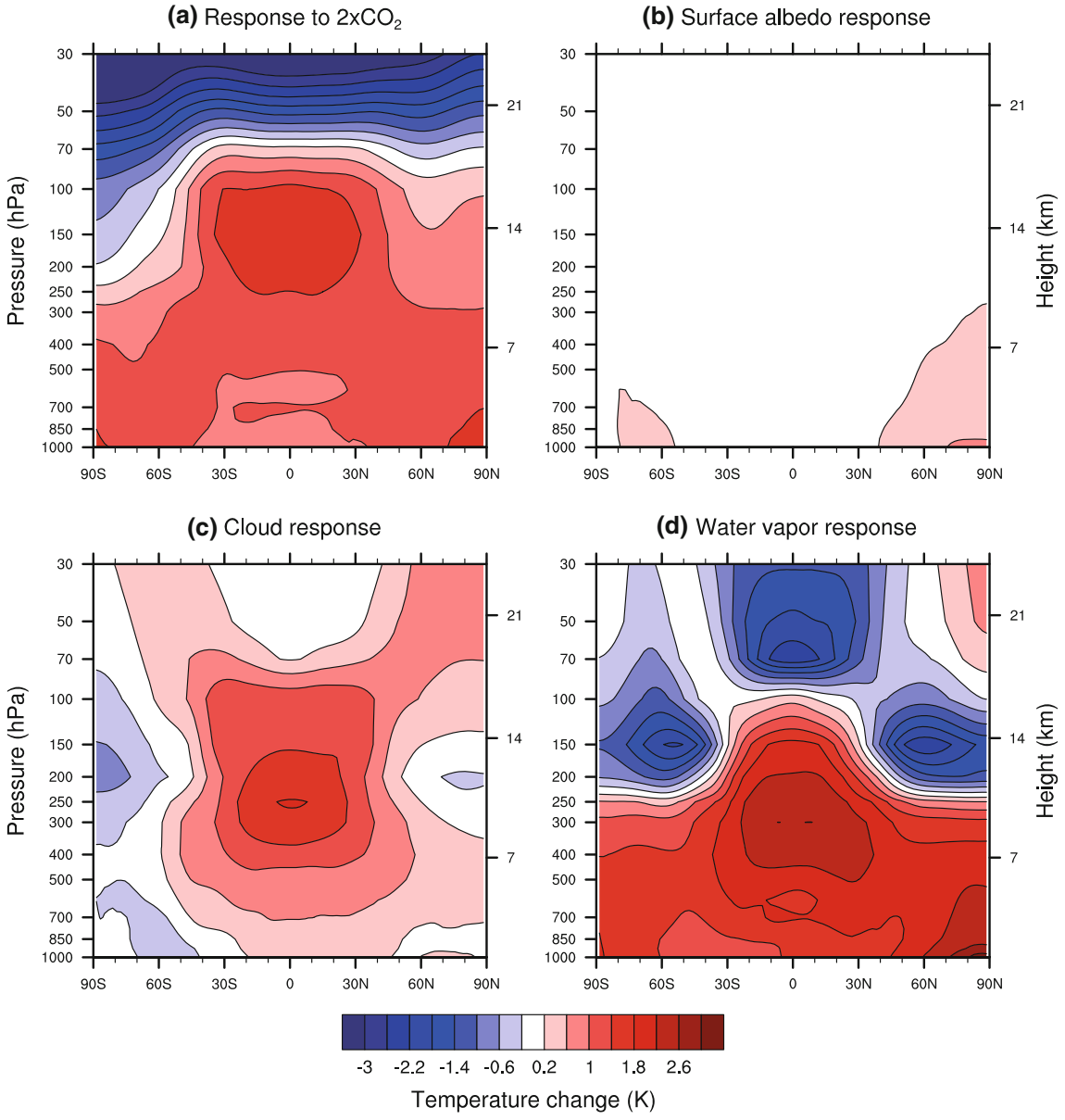

Fig. 8 Zonal average vertical structure of the response to climate change from CO_2 forcing, and the imposed surface albedo-, cloud-, and water vapor feedbacks

Having now determined the temperature response in the various model configurations, and estimated the relevant CO_2-forcing, we are now in a position to calculate the effective feedback factors according to the feedback analysis presented in Sect. 2 All effective feedback factors, along with those diagnosed using PRP, are given in Table 2. Overall, there is a striking similarity across the various estimates of feedback factors, in particular for the surface albedo and water vapor feedbacks, implying that indeed the assumptions of additivity and independence are reasonable approximations for many purposes. In what follows we shall seek to understand the main discrepancies.

4.2 Feedback efficiency

In the conceptual framework of the climate system it is assumed that feedback from the individual mechanisms can be added to yield the total system feedback. Put another way, it is assumed that each mechanism is equally capable—or efficient—in contributing to surface temperature change, and so there must be a constant ratio between radiative feedback and the associated partial temperature contribution. We can formalize this by defining the feedback efficiency as the ratio of the effective feedback factor, obtained from the temperature response when a feedback has been imposed on the climate system (Equation 4), to the diagnosed feedback obtained using the PRP-method (Table 2). This definition is analogous to the efficacy concept introduced for external forcings by Hansen et al. (2005). The feedback efficiencies are displayed in Fig. 7.

If the assumption of additivity is valid, then the feedback efficiency is unity for each feedback mechanism. This is closely fulfilled by the surface albedo and water vapor feedback mechanisms, both having efficiencies close to the ideal, despite the fact that they act very differently: The surface albedo feedback is a highly heterogeneous change in surface shortwave absorption peaking at high latitudes, while the water vapor feedback is a fairly homogenous change primarily in atmospheric longwave emissivity peaking in the tropics. Yet, in a global mean sense, the feedback from surface albedo and water vapor can simply be added in good agreement with what is frequently assumed. The cloud feedback, on the other hand, is particularly poor at inducing surface temperature change with a feedback efficiency of less than 40 percent. Thus, the assumption of additivity breaks down when the cloud feedback is considered.

The low efficiency of the cloud feedback must be understood from the structure of the temperature response, because temperature is the only variable that is permitted to influence radiation in this particular setup (Fig. 1c). Figure 8 shows the vertical structure of the partial temperature responses: The CO_2-forced temperature response is of tropospheric warming and stratospheric cooling, the surface albedo response is

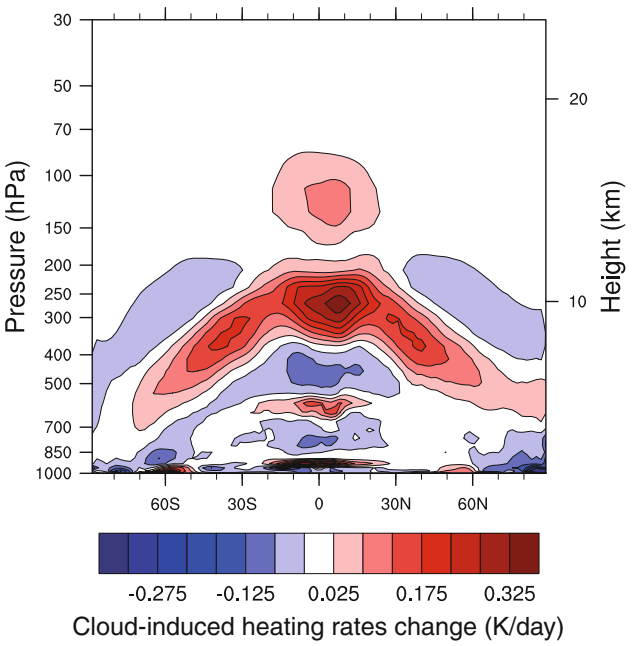

Fig. 9 Change in cloud-induced radiative heating rates diagnosed using PRP

bound to near-surface high-latitude warming and the water vapor response is that of cooling in the tropopause and lower stratosphere region and warming in the troposphere below. The cloud-induced warming that peaks below the tropical tropopause, also found by Wetherald and Manabe (1988) and Langen et al. (2012), coincides with a peak in the cloud-induced radiative heating (Fig. 9), that is likely due to enhanced longwave flux convergence associated with the rising of the tropopause: More longwave radiation is emitted from the surface in a warming climate, while the part of the skies that is covered with anvil clouds emit a roughly unchanged amount to space, which necessarily leads to longwave flux-convergence in the atmosphere below. This is particularly evident in the tropics, where cloud-induced warming aloft, unlike water vapor and CO_2, exceeds that of an effective moist adiabat (Fig. 10). The associated relative enhancement of the negative lapse-rate feedback due to clouds (warming aloft is more efficiently radiated to space than near-surface warming), is a physically appealing explanation for the weak cloud feedback efficiency. This is further supported by the strengthening of the total temperature feedback diagnosed from the full system (-4.05 W m^{-2} K^{-1}, Table 2) relative to the feedback-free system (-3.45 W m^{-2} K^{-1}), which is likely due to the identified cloud-induced warning in the upper troposphere.

4.3 Feedback synergies

We noted in the beginning of Sect. 4 that while the surface albedo and cloud feedbacks each contribute about the same

amount of surface temperature change, the drop in climate sensitivity when disabling only the cloud feedback is four times larger than when disabling only the surface albedo feedback (Fig. 5). This suggests that there is a positive synergy between the cloud- and water vapor feedbacks. In other words, the combined feedback is greater than the sum of its parts. We may define the synergy (S) between the cloud- and water vapor feedbacks as:

$$S_{C+W} = \lambda_{CW} - (\lambda_C + \lambda_W),$$

where the λ's are obtained from simulations with one or two locked feedback mechanisms (Table 2, Eqs. 7 and 6).

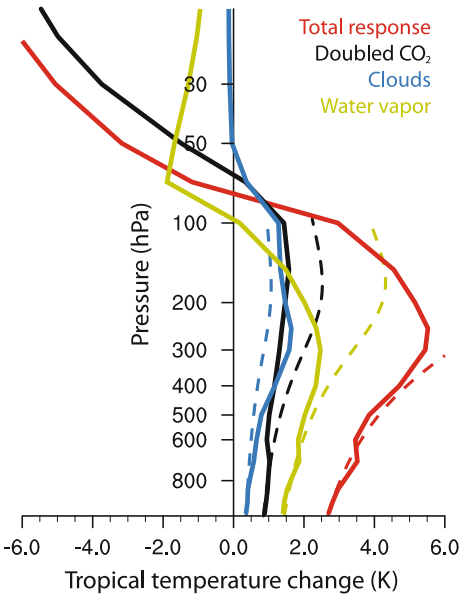

Fig. 10 Vertical structure of warming in the tropics (30S–30N). *Full lines* are the temperature responses to the respective imposed feedbacks mechanisms. *Dashed lines* are moist adiabats corresponding to the surface temperature change pertaining to each feedback mechanism

Positive S indicates that interactions between the feedbacks act to strengthen climate change beyond that predicted by assuming independence of the feedback processes. Evaluating S_{C+W} indeed yields a positive synergy of +0.15 W m^{-2} K^{-1} (Fig. 11a). Off-line PRP calculations confirm that the positive synergy is not a consequence of pure radiation interactions, but occurs because of changes in the atmospheric state; in this case temperature, water vapor and clouds can change. The positive synergy between clouds and water vapor raises the climate sensitivity of the climate system from 2.41 K, predicted from Eq. (2) by adding the feedback factors when the mechanism act in isolation ($-F/(\lambda_T + \lambda_W + \lambda_C)$), to 2.71 K when they are allowed to interact ($\Delta\widetilde{T}_{CW}$). One possible explanation for the positive synergy is that the cloud-induced warming in the upper Tropical troposphere permits a higher specific humidity, provided the relative humidity does not change much, thereby increasing the strength of the water vapor feedback. Water vapor in this part of the atmosphere is particularly effective in reducing the outgoing longwave radiation (Held and Soden 2000).

A synergy between a single feedback and the combination of two is calculated analogously, e.g. $S_{A+CW} = \lambda_{ACW} - (\lambda_A + \lambda_{CW}) = -0.17$ Wm^{-2}K^{-1} (Fig. 11a). All the six synergies between the possible combinations of the three studied feedback mechanisms are displayed in Fig. 11b. The surface albedo feedback exhibits negative synergies with the water vapor and cloud feedbacks, both individually and in combination. Adding the albedo feedback factor to the combined cloud and water vapor feedback should have raised the global climate sensitivity to 3.38 K from the 2.71 K without the surface albedo feedback ($\Delta\widetilde{T}_{CW}$). However, negative synergies surrounding the surface albedo feedback act to reduce the global climate sensitivity by 0.47 K to merely 2.91 K (ΔT).

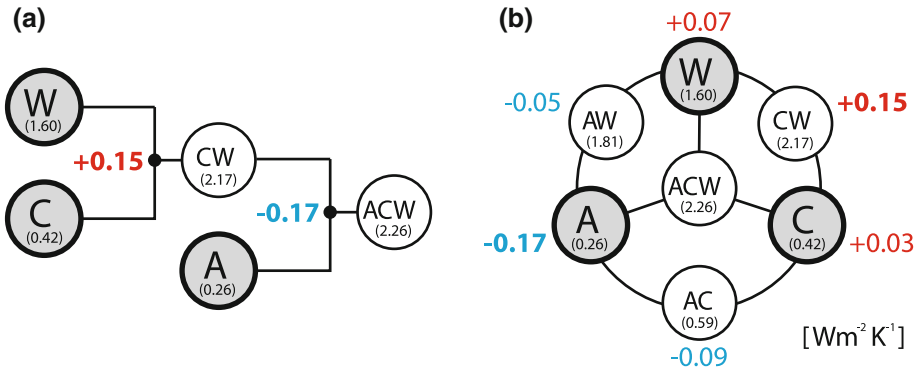

Fig. 11 Feedback synergy example **a** where first cloud and water vapor feedbacks combine with positive synergy, then when further adding surface albedo there is negative synergy, and **b** a summary of all feedback synergies shown as *red* and *blue numbers* around the rim of the *circle*. *Bold numbers* represent the same synergies in **a** and in **b**. *Small black numbers* below each feedback, or combination of feedbacks, are respective feedback factors repeated from Table 2 evaluated using Eqs. (6–7), with the exception of the feedback of all three mechanisms combined which is calculated as $\lambda_{ACW} = \lambda - \lambda_T$

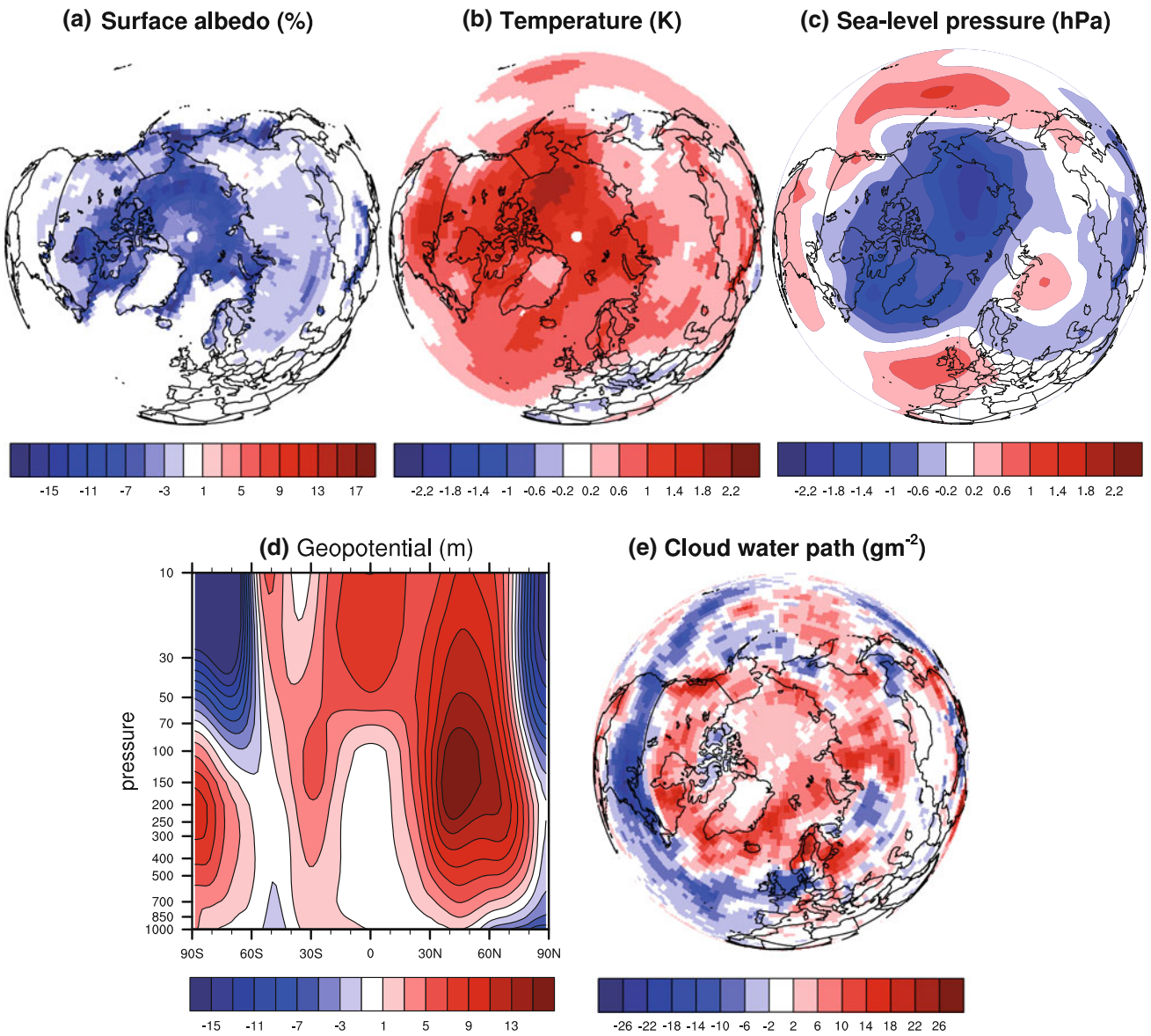

Fig. 12 Impacts of changing surface albedo. **a** Shows the effective change in surface albedo calculated from the annual mean surface shortwave radiation budget in the standard simulations ($2xCO_2$ minus CTRL). **b–e** Show change between the standard simulations and those with locked albedo ($2xCO_2$-A1 minus $1xCO_2$-A1)

It is sometimes argued that near-surface warming in the Arctic due to sea-ice melt permits increased lower tropospheric water vapor and thereby further warming (Screen and Simmonds 2010; Serreze and Barry 2011). Although more water vapor in the lower troposphere will increase the downwelling longwave radiation towards the surface leading to local surface warming, it also leads to an increase in the longwave radiation to space because the lower troposphere is usually warmer than the surface at high latitudes (Soden et al. 2008). Therefore, somewhat counter to intuition, likely the interaction between atmospheric water vapor and sea ice melt is to reduce the anticipated global mean climate change.

The negative synergy between surface albedo and clouds is likely associated with circulation changes as can be inferred from Fig. 12. Here the influence of the surface albedo feedback is derived from simulations with and without the feedback active ($2xCO_2$–CTRL versus $2xCO_2$-A1–$1xCO_2$-A1). The warming associated with the declining surface albedo induces high-level divergence, rising motion, and a decrease of sea-level pressure over the Arctic Ocean and North Atlantic, all of which is consistent with a direct thermal cell responding to surface warming. The altered circulation results in a thickening of the cloud deck at high latitudes and a thinning at mid-latitudes (Fig. 12e), the net effect of which is likely a weakening by clouds of

the surface temperature change originating from the surface albedo feedback.

5 Conclusions

We have investigated the validity of assuming additivity and independence of feedback mechanisms—assumptions that are fundamental to the current framework for understanding the role of feedback mechanisms in the climate system. This was done by systematically controlling the state of the water vapor, cloud and surface albedo feedbacks in a climate model. We show that by imposing the feedbacks, one by one, we obtain a near-perfect decomposition of climate change into responses pertaining to each feedback mechanism.

The correspondence between the diagnosed top-of-atmosphere radiative feedback and the surface temperature response for the three feedback mechanisms, was studied by defining a feedback efficiency, which is the ratio of the effective feedback factor derived from the temperature response to the diagnosed feedback factor. Both the water vapor and surface albedo feedbacks have efficiencies close to unity, in good agreement with the assumption of additivity. The cloud feedback, on the other hand, is highly inefficient and contributes less than 40 percent of the anticipated surface temperature change predicted by theory. The weak cloud feedback efficiency is likely a consequence of the stronger than moist-adiabatic cloud-induced warming in the upper parts of the tropical troposphere that enhance the negative lapse-rate feedback, thereby off-setting a large part of the anticipated surface warming. The warming pattern is consistent with the idea that anvils of convective clouds rise under global warming, leading to atmospheric flux-convergence and warming predominantly aloft.

We further find that the combined cloud and water vapor feedback is greater than the sum of its parts, while the response to the surface albedo feedback is dampened relative to expectation by the associated cloud and water vapor change. The implied feedback synergies result in appreciable changes to climate sensitivity. For example, the negative synergies erode most of the anticipated climate sensitivity increase from adding the surface albedo feedback to the climate system from 0.67 K, down to only 0.20 K. The synergies pertaining to water vapor feedback can be understood from the vertical structure of warming, as the cloud-induced warming in the cold upper tropical troposphere permits more water vapor where it is the most efficient in reducing outgoing longwave radiation. Conversely, the near-surface warming at high latitudes associated with the surface albedo feedback likely has a near-zero impact on the water vapor feedback because the lower troposphere is on average warmer than the surface. In addition, the thickening of clouds at high latitudes associated with decreasing surface albedo, which can be understood from changes in the atmospheric circulation, act to further dampen climate change.

In summary, we find that the simple energy balance model central to the current conceptual framework of the climate system is generally applicable when considering the temperature, water vapor and surface albedo feedbacks. Although we find a weak negative synergy between the water vapor and surface albedo feedbacks (-0.05 W m^{-2} K^{-1}), this hardly matters for the global mean climate sensitivity. However, the conceptual framework is challenged when clouds are considered: Cloud feedback is ineffective in contributing to surface temperature change on its own, while cloud interaction with water vapor through atmospheric lapse-rate change acts to strengthen climate sensitivity. The results highlight the need to understand and consistently treat the coupling between clouds, water vapor and lapse-rate in a deepening troposphere.

Discussions with and comments from Robert Pincus, Isaac Held, Sandrine Bony, Jean-Louis Dufresne, David Battisti, Aiko Voigt, Jürgen Bader, Jianhua Lu and an anonymous reviewer were valuable in advancing our study. This study was supported by the Max-Planck-Gesellschaft (MPG), funding through the EUCLIPSE project from the European Union, Seventh Framework Programme (FP7/2007-2013) under grant agreement no 244067, and computational resources were made available by Deutsches Klimarechenzentrum (DKRZ) through support from Bundesministerium für Bildung und Forschung (BMBF).

References

Arrhenius S (1896) On the influence of carbonic acid in the air upon the temperature of the ground. J Sci 41:237–275

Augustsson T, Ramanathan V (1977) A radiative-convective model study of the CO_2 climate problem. J Atm Sci 34:448–451

Block K, Mauritsen T (2013) Forcing and feedback in MPI-ESM-LR coupled model after quadrupled CO_2. J Adv Model Earth Syst (in press)

Cess RD et al (1990) Intercomparison and interpretation of climate feedback processes in 19 atmospheric general circulation models. J Geophys Res 95:16601–16615

Cess RD et al (1991) Interpretation of snow-climate feedback as produced by 17 general circulation models. Science 253:888–892

Colman RA, McAvaney BJ (1997) A study of general circulation model climate feedbacks determined from perturbed sea surface

temperature experiments. J Geophys Res 102(D16):19383–19402. doi: 10.1029/97JD00206
Colman RA (2003) Comparison of climate feedbacks in general circulation models. Clim Dyn 20:865–873
Colman RA, McAvaney BJ (2011) On tropospheric adjustment to forcing and climate feedbacks. Clim Dyn 36:1649–1658
Crook JA, Forster PM, Stuber N (2011) Spatial patterns of modeled climate feedback and contributions to temperature response and polar amplification. J Clim 24:3575–3592
Dufresne J-L, Bony S (2008) An assessment of the primary sources of spread of global warming estimates from coupled atmosphere–ocean models. J Clim 21(1):5135–5144. doi: 10.1175/2008JCLI2239
Giorgetta M et al (2013) Climate variability and climate change in MPI-ESM simulations. J Adv Model Earth Syst, submitted
Graversen RG, Wang M (2009) Polar amplification in a coupled climate model with locked albedo. Clim Dyn 33:629–643. doi: 10.1007/s00382-009-0535-6
Gregory JM, Ingram WJ, Palmer MA, Jones GS, Stott PA, Thorpe RB, Lowe JA, Johns TC, Williams KD (2004) A new method for diagnosing radiative forcing and climate sensitivity. Geophys Res Lett 31:L03205. doi: 10.1029/2003GL018747
Gregory J, Webb M (2008) Tropospheric adjustment induces a cloud component in CO_2 forcing. J Clim 21:58–71
Hall A (2004) The role of surface albedo feedback in climate. J Clim 17:1550–1568
Hall A, Manabe S (1999) The role of water vapor feedback in unperturbed climate variability and global warming. J Clim 12:2327–2346
Hansen J, Sato M, Ruedy R (1997) Radiative forcing and climate response. J Geophys Res 102(D6):6831–6864
Hansen J, SatoMki , Ruedy R, Nazarenko L, Lacis A, Schmidt GA, Russell G, Aleinov I, Bauer M, Bauer S, Bell N, Cairns B, Canuto V, Chandler M, Cheng Y, Del Genio A, Faluvegi G, Fleming E, Friend A, Hall T, Jackman C, Kelley M, Kiang NY, Koch D, Lean J, Lerner J, Lo K, Menon S, Miller RL, Minnis P, Novakov T, Oinas V, Perlwitz JP, Perlwitz Ju, Rind D, Romanou A, Shindell D, Stone P, Sun S, Tausnev N, Thresher D, Wielicki B, Wong T, Yao M, Zhang S (2005) Efficacy of climate forcings. J Geophys Res 110:D18104. doi: 10.1029/2005JD005776
Hartmann DL, Larson K (2002) An important constraint on tropical cloud–climate feedback. Geophys Res Lett 29. doi: 10.1029/2002GL015835
Held IM, Soden BJ (2000) Water vapor feedback and global warming. Annu Rev Energy Environ 25:441–475
Held IM, Shell KM (2012) Using relative humidity as a state variable in climate feedback analysis. J Clim 25:2578–2582. doi: JCLI-D-11-00721.1
Ingram W (2013) A new way of quantifying GCM water vapor feedback. Clim Dyn 40:913924. doi: 10.1007/s00382-012-1294-3
Jonko AK, Shell KM, Sanderson BM, Danabasoglu G (2012) Climate feedbacks in CCSM3 under changing CO_2 forcing. Part II: variation of climate feedbacks and sensitivity with forcing. J Clim. doi: 10.1175/JCLI-D-12-00479.1
Klocke D, Quaas J, Stevens B (2013) Assessment of different metrics for physical climate feedbacks. Clim Dyn. doi: 10.1007/s00382-013-1757-1
Langen PL, Graversen RG, Mauritsen T (2012) Separation of contributions from radiative feedbacks to polar amplification on an aquaplanet. J Clim. doi: 10.1175/JCLI-D-11-00246.1
Lu J, Cai M (2009) A new framework for isolating individual feedback processes in coupled general circulation climate models. Part I: formulation. Clim Dyn. 32:873885. doi: 10.1007/s00382-008-0425-3
Manabe S, Wetherald RT (1967) Thermal equilibrium of the atmosphere with a given distribution of relative humidity. J Atm Sci 24:241–59
Randall DA, et al (1994) Analysis of snow feedbacks in 14 general circulation models. J Geophys Res 99, D10,20,757–20,771
Schneider EK, Kirtman BP, Lindzen RS (1999) Tropospheric water vapor and climate sensitivity. J Atm Sci 56:1649–1658
Screen JA, Simmonds I (2010) The central role of diminishing sea ice in recent Arctic temperature amplification. Nature 464:1334–1337
Serreze MC, Barry RG (2011) Processes and impacts of Arctic amplification: a research synthesis. Global Planet Change 77:85–96
Solomon S, et al (2007) Contribution of Working Group I to the Fourth Assessment Report of the Intergovernmental Panel on Climate Change
Soden BJ, Held IM (2006) An assessment of climate feedbacks in coupled ocean–atmosphere models. J Clim 19:3354–3360
Soden BJ, Held IM, Colman R, Shell KM, Kiehl JT, Shields CA (2008) Quantifying climate feedbacks using radiative kernels. J Clim 21:3504–3520
Stevens B et al (2013) Atmospheric component of the MPI-M earth system model: ECHAM6. J Adv Model Earth Syst. doi: 10.1002/jame.20015
Taylor KE, Stouffer RJ, Meehl GA (2012) An overview of CMIP5 and the experiment design. Bull Am Meteorol Soc 93:485–498
Vial J, Dufresne J-L, Bony S (2013) On the interpretation of inter-model spread in CMIP5 climate sensitivity estimates. Clim Dyn. doi: 10.1007/s00382-013-1725-9
Webb MJ, Hugo Lambert F, Gregory JM (2013) Origins of differences in climate sensitivity, forcing and feedback in climate models. Clim Dyn 40:677707. doi: 10.1007/s00382-012-1336-x
Wetherald RT, Manabe S (1988) Cloud feedback processes in a general circulation model. J Atmos Sci 45:1397–1415
WMO (1992) International meteorological vocabulary (2nd edn). Secretariat of the World Meteorological Organization, Geneva, p 636. ISBN 92-63-02182-1
Zelinka MD, Hartmann DL (2010) Why is longwave cloud feedback positive? J Geophys Res 115:D16117. doi: 10.1029/2010JD013817